Role of Ions on Structure and Stability of a Synthetic Gramicidin Ion Channel in Solution. A Molecular Dynamics Study

Giulia Morra,[†] Ulrich Koert,[‡] and Ernst-Walter Knapp*[,†]

Department of Biology, Chemistry and Pharmacy, Institute of Chemistry, Freie Universität Berlin, Takustrasse 6, 14195 Berlin, Germany, and Department of Chemistry, Philipps-Universität Marburg, Marburg, Germany

Received: December 21, 2004; In Final Form: March 12, 2005

We performed a molecular dynamics (MD) simulation to the investigate structure and stability of a synthetic gramicidin-like peptide in solution with and without ions. The starting structures of the MD simulations were taken from two recently solved NMR structures of this peptide in isotropic solution, which forms stable monomers or dimers in the presence or absence of ions, respectively. The monomeric structure is channel-like and is assumed to be stabilized by the presence of two Cs^+ ions bound in the channel, each one close to one channel entrance. In our MD simulations, we observed how the Cs^+ ions bind in the channel formed by the monomeric gramicidin-like peptide using implicit solvent and explicit ions with a concentration of 2 M. MD simulations were performed with and without explicit ions but with an implicit solvent model defined by the generalized Born approximation, which was used to mimic the dielectric properties of the solvent and to speed up the computations.

Introduction

Gramicidin A is a hydrophobic polypeptide of 15 amino acids synthesized by *Bacillus brevis*, which has a variety of biological activities, being antibiotic,[1] antiviral, and spermicidal.[2] It forms a helical structure in membranes, which is active as an ion channel and selective for monovalent cations. Thus, the antibiotic activity is performed by increasing the cation permeability in biological membranes.[3]

Gramicidin A can adopt different conformations depending on the environment. In organic solvents, it adopts either a monomeric random coil structure or a β-helical double-stranded dimer structure with different topologies and left- or right-handed orientations.[4−6] In lipid bilayer membranes, gramicidin A assumes a completely different fold, namely, the structure of the active ion channel. It is built by two gramicidin A polypeptides, which are associated head to head in opposite halves of the lipid bilayer where they form right-handed single-stranded helices.[7,8] Because of the known tertiary structure, gramicidin A was extensively investigated theoretically to elucidate both the equilibrium structural properties[8,9,17] and the mechanism and energetics of ion permeation and selectivity.[10−14]

Gramicidin A can be modified by molecular engineering. Its activity is detected in real time by measuring the current across a membrane. It is an actual research field to consider the functional unit of two gramicidin helices, which are pairwise bridging a lipid bilayer membrane, as a template to construct synthetic ion channels.[15] Along these lines, Arndt et al.[16] recently produced the synthetic polypeptide **1** obtained by joining two 11 amino acid containing sequences of gramicidin A head to head via a succinyl linker and studied its properties. Electrophysiological measurements showed that this polypeptide is active as ionic channel when placed in a lipid bilayer membrane. The synthetic gramicidin-derived polypeptide 1 was investigated also in isotropic solution by means of NMR spectroscopy to elucidate its structural properties. In organic solvents consisting of benzene/acetone 10:1 or chloroform/methanol 1:1 mixtures, the polypeptide 1 adopts a dimeric, double-stranded helical conformation (Figure 2, top panel, NMR average structure).[16] These left-handed helices are narrow and shifted into each other such that they do not possess a pore, albeit they involve 5.7 amino acids per turn. Interestingly, this double-stranded helix structure undergoes a conformational transition in a solution saturated with cesium iodide. Here, the synthetic gramicidin-derived polypeptide 1 assumes the structure of a monomeric right-handed, single-stranded helix with a pore of diameter 4.5 Å, involving 6.3 amino acids per turn. This structure can be considered the equivalent to the active channel-like conformation of natural gramicidin A in membranes, since it actually shows ion-conducting activity in the Cs^+-enriched solution.[16] According to the experimental data, it is proposed that adding cations to the solution triggers the dissociation of the double-stranded helix, such that each single chain forms a single-stranded helix. This structure is supposed to be stabilized by binding subsequently two Cs^+ ions at both ends.

The aim of this work is to investigate by molecular dynamics (MD) simulations the properties of double- and single-stranded helical structures that are adopted by the synthetic gramicidin-like polypeptide **1** in ionic solution. We simulate both structures in the absence and in the presence of Cs^+ ions, to explore stability and conformational changes due to the interaction with ions. Moreover, we simulated the binding reaction of two Cs^+ ions in the pore of the monomeric single-stranded helical structure. Thereby, the binding of the second Cs^+ ion is particularly interesting because of the strong electrostatic repulsion relative to the first bound ion.

Materials and Methods

Structures. The monomeric unit of the synthetic mini-gramicidin A (polypeptide **1)** consists of two copies of the terminal 11 amino acids of the native gramicidin A (Figure 1).

* Author to whom correspondence should be addressed. E-mail: knapp@chemie.fu-berlin.de

[†] Freie Universität Berlin.

[‡] Philipps-Universität Marburg.

10.1021/jp044191u CCC: $30.25
Published on Web 04/26/2005

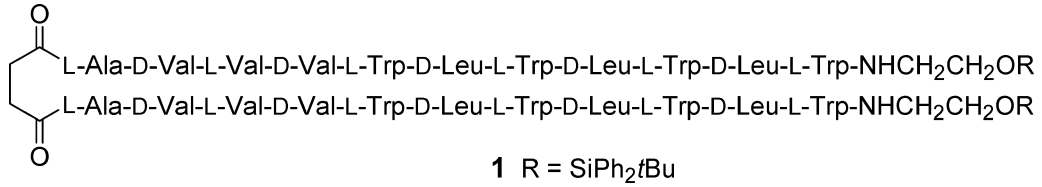

Figure 1. Sequence of the synthetic polypeptide **1**.

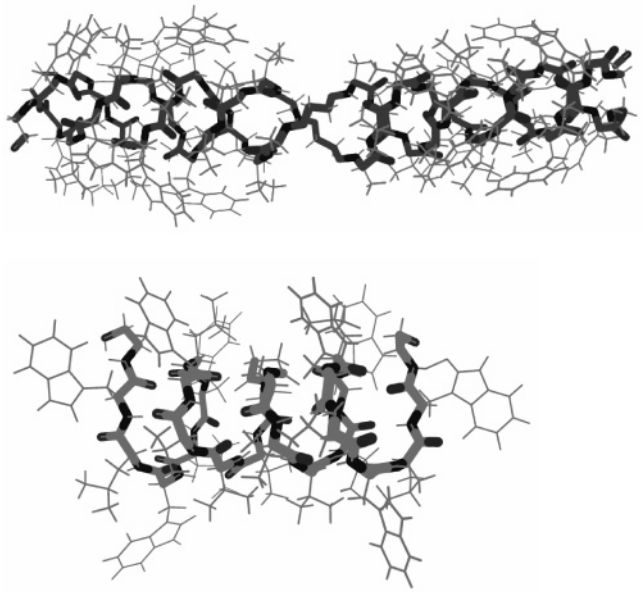

Figure 2. NMR structures of the artificial gramicidin dimer (top panel, PDB entry 1KQE) and monomer (bottom panel).[16] The figure was generated using MOLSCRIPT.[29]

These two segments are covalently connected head to head via a succinic acid molecule. The resulting monomer structure consists thus of 22 amino acids and a succinyl linker. Each segment contains hydrophobic residues only, namely, tryptophane, alanine, leucine, and valine but also D-leucine and D-valine. The dimer is made of two monomers forming a double helix (Figure 2). In the following, we refer to the double-stranded helix as the dimer structure and to the single-stranded helix as the monomer structure. The NMR structure of the double-stranded helix (PDB code 1KQE, Figure 2, top panel) was used as the starting conformation in the MD simulation of the dimer. The NMR structure of the single-stranded monomer as given in ref 16 is displayed in Figure 2, bottom panel. The terminal *tert*-butyl-triphenyl-silyl (TBDPS) groups attached to the ethanolamine ends of polypeptide **1** to improve solubility could not be detected by NMR spectroscopy, presumably due to their high flexibility. Since these groups do not belong to the central part of the mini-gramicidin structure and do not adopt a definite conformation, we neglect them in our calculations.

General Setup of Molecular Dynamics. For the molecular dynamics simulations, the program CHARMM[18] was used, with the parameters given by the CHARMM22 set.[19] In the case of ethanolamine, partial charges were calculated from the electronic wave functions obtained in the Hartree−Fock approximation with the 6-31G* basis set by fitting the resulting electrostatic potential in the neighborhood of these molecules with the restrained electrostatic potential model [20] (Supporting Information). The time propagation of the MD trajectories was performed with the velocity Verlet algorithm implemented in CHARMM, with the temperature kept constant at 300 K by means of the Nose−Hoover thermostat.[21,22]

The solvent was treated implicitly by the generalized Born approximation[23] using the corresponding generalized Born with simple switching (GBSW) module recently implemented in CHARMM.[24] Since the NMR structure determinations were performed in a 1:1 mixture of methanol/chloroform, we used in the simulations a solvent dielectric constant of $\epsilon = 20$, which is slightly higher than the average of the dielectric constants of methanol ($\epsilon = 32.6$) and chloroform ($\epsilon = 4.8$). One can assume that the solvation properties of the solution are mainly determined by its polar component, namely, methanol, resulting in an effective dielectric constant that is higher than values typical for membranes under physiological conditions.

The generalized Born parameters of GBSW were adjusted using $\epsilon = 1$ for solute and $\epsilon = 80$ for solvent. Unfortunately, there is no GBSW parametrization for different dielectric constants available as needed in the present application. However, since we focus on molecular geometries and not energies, the results computed from the MD simulations are likely to be meaningful. In the present study, the dielectric constant of the solute was set to $\epsilon = 4$. Values higher than $\epsilon = 1$ were chosen to account for electronic polarizability.[25,26] Using a lower dielectric constant of $\epsilon = 2$ did not provide qualitative changes in the results, albeit the mini-gramicidin structures exhibited more fluctuations than with $\epsilon = 4$ (Figure S3 of the Supporting Information). When MD simulations of the monomeric synthetic gramicidin including ions were performed at $\epsilon = 1$, it was not possible to simultaneously keep two Cs^+ ions inserted at both ends of the channel because they strongly repelled each other. In the following, we refer to MD simulations that are based on the implicit solvent model with generalized Born using $\epsilon = 20$ for the solvent and $\epsilon = 4$ for polypeptide **1**. The monomer structure was simulated in the absence and in the presence of two bound Cs^+ ions. Note that with implicit solvent the energetics of ion solvation by explicit solvent molecules are taken care of qualitatively by the interaction of the solute with the dielectric boundary. Explicit solvent structure at the Cs^+ ion solvation shell may significantly alter the energy balance between solvated and channel-bound Cs^+ ions but not the geometry of the bound ions.

Generating Cs^+ Ion Coordinates in the Channel. To obtain optimized initial positions for the Cs^+ ions, we first generated an energy trace of the Cs^+ ion by moving it in steps of 0.5 Å along the channel axis and optimizing for each fixed ion position the polypeptide atoms by energy minimization with 1000 steps of steepest descent (SD) followed by 1000 steps with the adopted basis Newton−Raphson (ABNR) algorithm. In this way, we also probed Cs^+ ion positions at both channel entrances, since the monomer structure extends by about 20 Å along the channel axis whose total length is 40 Å. These energy traces were computed using the CHARMM22 [19] potential energy in vacuum and with the generalized Born implicit solvent model GBSW of CHARMM[24] and displayed as solid lines in Figure 3 top, left and right panels, respectively. Under vacuum conditions, the energy trace showed a funnel-like behavior at both channel entrances, resulting in an attractive potential guiding the ion in the channel interior, compatible with easy

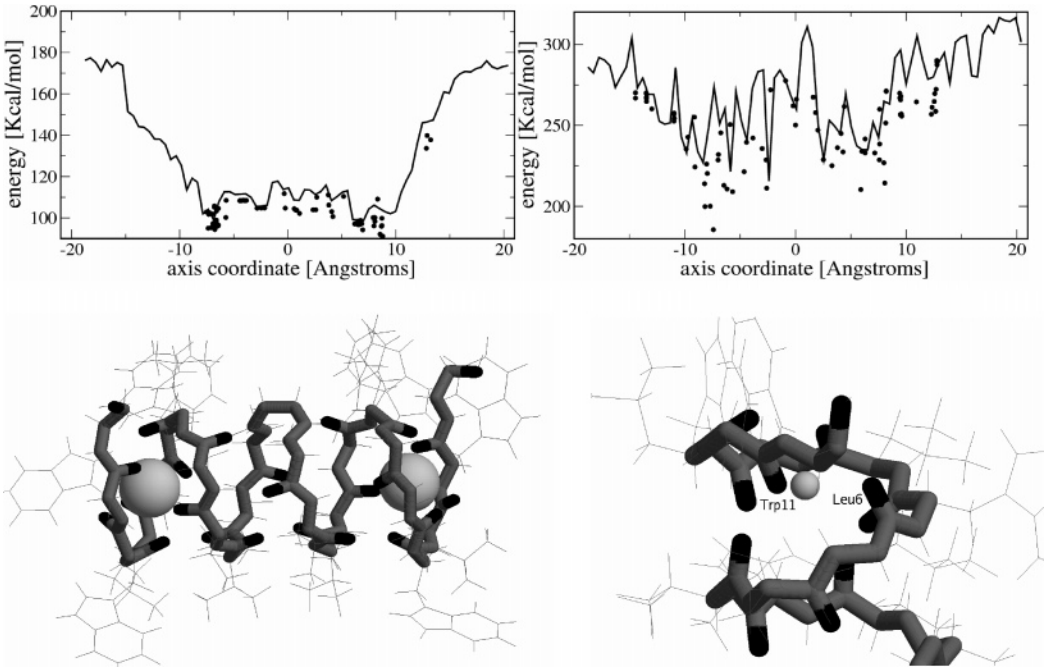

Figure 3. Cs^+ ion position in the polypeptide **1** monomer structure. Top panels: Energy trace obtained by moving a Cs^+ ion along the channel axis of 40 Å in length in steps of 0.5 Å (number of steps, 80) using the CHARMM22 vacuum energy function (left panel) and the GBSW energy function accounting for implicit solvent (right panel). At each ion position, the polypeptide structure is relaxed by energy minimization with fixed ion position yielding the energy profile (solid line). The ion position is further energy-minimized, first by keeping the polypeptide fixed, then by relaxing the polypeptide and ion structure without constraints. The resulting energy values and ion axis coordinates are displayed as black dots in the plot. For more details, see text. Bottom panels: Two views of the binding sites, showing the interaction with the backbone oxygen atoms of Trp11 and Leu6. Figures were generated using Rasmol.[27]

ion binding. For the interior of the channel, the ion experienced a succession of energy minima and maxima with deep minima in the vicinity of both channel entrances. We used these channel structures with Cs^+ ion positions along the channel axis as starting points of further energy minimizations with 200 steps of SD followed by 200 steps with ABNR. During this energy minimization, the Cs^+ ion can now leave the channel axis, while the polypeptide atoms are immobilized in the previously obtained optimized structure. Finally, polypeptide and ion were energy-minimized without constraints (800 SD and 800 ABNR steps), leading to a number of energy minima that are marked by dots in the top panels of Figure 3.

The computed energy values of the ion in the channel (dots in Figure 3) may deviate considerably from the energy trace (solid line), since they are obtained by a subsequent unconstrained minimization of the polypeptide and ion. However, the final ion positions are close to the energy minima locations along the energy trace. In particular, in about half of all energy minimizations, the final ion positions fall in the vicinity of one of the deep minima at the channel axis coordinates $x = 6.5$ Å and $x = -6.5$ Å At these positions are the two putative binding sites of the Cs^+ ions in the channel. The same calculations performed with the implicit solvent model energy function led to a similar energy profile, Figure 3, right panel. Here, a more rugged energy profile was found in the channel interior, whose overall shape is still downhill from the channel entrance toward the internal region. The optimal ion positions obtained after unconstrained energy minimization are correspondingly more spread than in the vacuum calculation, with deep energy values located at axis coordinates around $x = 6.5$ Å and $x = -6.5$ Å. Thus, to perform MD simulations of the synthetic ion channel, we employed as initial Cs^+ ion positions the coordinates $x = 6.5$ Å and $x = -6.5$ Å on the channel axis, corresponding to the most occupied Cs^+ ion positions after optimization in vacuum. To relax the molecular system in the presence of two Cs^+ ions with their repulsive interaction, several minimization cycles (50 SD steps for the Cs^+ ions with fixed protein atoms, 50 SD and 100 ABNR steps for the polypeptide backbone only, and 50 SD and 100 ABNR steps for all atoms) were performed before the MD simulation was started. These ion positions are shown in Figure 3, bottom panels. The Cs^+ ion in the channel is close to the Trp11 and Leu6 backbone oxygens (Figure 3, bottom, right panel). Note, however, that the Cs^+ ion penetration in the synthetic gramicidin depends crucially on the relatively polar solvent environment modeled by a dielectric medium with $\epsilon = 20$ that differs considerably from a membrane environment as discussed before.

MD Simulations with Implicit Solvent. In a series of MD simulations, both solvent and ions were modeled implicitly by setting the ionic strength to 1 M in the GBSW module. In preliminary calculations, we tried also implicit ionic strength values from 0.1 to 10 M, without observing qualitative changes in the stability of the monomer and dimer structures. The value of 1 M reflects experimental conditions where Cs^+ ion binding is supposed to take place in the monomer. In a second series of calculations, Cs^+ and I^- ions were modeled explicitly in a cubic box of $53 \times 53 \times 53$ Å^3 with periodic boundary conditions. A homogeneous distribution of ions was generated by placing Cs^+ and I^- ions randomly on grid points of a cubic lattice with a 6 Å distance corresponding to an ion concentration of 2 M. The resulting distribution was then modified to acquire charge neutrality. The molecular system was placed in the center of this ion bath. Excess ions at a distance smaller than 4 Å from any atom of the molecular system were removed. The ion positions were first optimized with the fixed molecular system (100 SD steps followed by 2000 ABNR steps), and then the total system was energy-minimized (100 SD and 300 ABNR steps) before the MD simulation was started. The use of explicit ions has the advantage to take into account

fluctuations of ionic concentration, which may result in additional interactions that stabilize or destabilize the monomeric structure.

In MD simulations with the implicit solvent model and explicit ions, a major problem was to keep the distribution of ions sufficiently uniform. The ions tended to cluster because of their strong electrostatic interaction, which was not enough shielded by a dielectric medium with $\epsilon = 20$ representing the implicit solvent. To reduce the tendency of ion clustering and to keep the ionic distribution more uniform, we increased the van der Waals radius of the iodine ions and doubled their number while simultaneously reducing their charge to half of a unit charge, thus maintaining charge neutrality and ionic strength. However, since we wanted to observe the Cs^+ ion binding in the channel, we did not change those parameters for the MD simulation. Both changes of the iodine ion parameters reduced the Cs−I ion attraction and thus contributed to a homogeneous ion distribution. Thus, the ion concentration of 2 M corresponding to the maximum value used in the experiments to study the monomer structure in ref 16 was modeled by 157 Cs^+ and 314 I^- ions, the latter with half a unit charge. After a number of test runs, the radius of the negatively charged I^- ions was set to 4.4 Å, as compared to the standard value of 2.35 Å used in the AMBER force field.[28] This value turned out to be large enough to keep the ion distribution sufficiently homogeneous. The Cs^+ ion radius was set to the van der Waals value of 3.395 Å, as taken from the AMBER force field,[28] which was used as the Born radius.

A set of 10 MD trajectories with the implicit solvent model at $T = 300$ K and without ions, each extending to 1 ns, were calculated for the dimer and monomer structures. In the presence of two Cs^+ ions, the monomer was also simulated using the same procedure but with an implicit ionic strength of 1 M to account for the ionic strength applied in experiments. For each species, 1 out of these 10 trajectories was extended by another 1 ns and used for graphical display.

In the case of MD simulations with a bath of explicit ions under periodic boundary conditions, we calculated a set of 10 MD trajectories at $T = 300$ K, with implicit solvent, in a cubic box of $53 \times 53 \times 53$ Å^3 with periodic boundary conditions involving a total number of 923 atoms. Each of these trajectories amounts to 2 ns, resulting in a total simulation time of 20 ns. All trajectories within the same set have the same initial conditions but a different random seed used for generating the initial velocity distribution.

Analysis of MD Simulation Data. The conformational root-mean-square (rms) deviation of the MD simulation data was calculated with respect to the initial minimized structure considering backbone atoms only, according to the equation

$$\langle \Delta \vec{r}(t) \rangle = \left(\frac{1}{N} \sum_{i=1}^{N} (\vec{r}_i(t) - \vec{r}_i^{\,\mathrm{init}})^2 \right)^{1/2} \qquad (1)$$

where global displacement and orientation are removed. The index i runs over the set of backbone atoms, $\vec{r}_i(t)$ indicates the position of the ith atom at time t, and the label init refers to the initial conformation.

Results

Monomer and Dimer Structure in Absence of Ions. Monomer and dimer structures were simulated at $T = 300$ K in the absence of ions. To make sure that the MD simulation data reflect the typical dynamical behavior of the considered molecular system, we generated for both systems 10 trajectories each of 1 ns time length, yielding a total time of 10 ns. However, detailed results from these data were displayed for one of these trajectories, which was prolonged to 2 ns. The aim of these calculations was to compare the persistence of the monomer and dimer structures, as an indication of the stability of both conformations, to confirm that the dimer structure is indeed in the preferred conformation in the absence of ions as found in the experiments. The analysis of rms deviations (eq 1) was used as a criterion to distinguish between stable and less stable conformations.

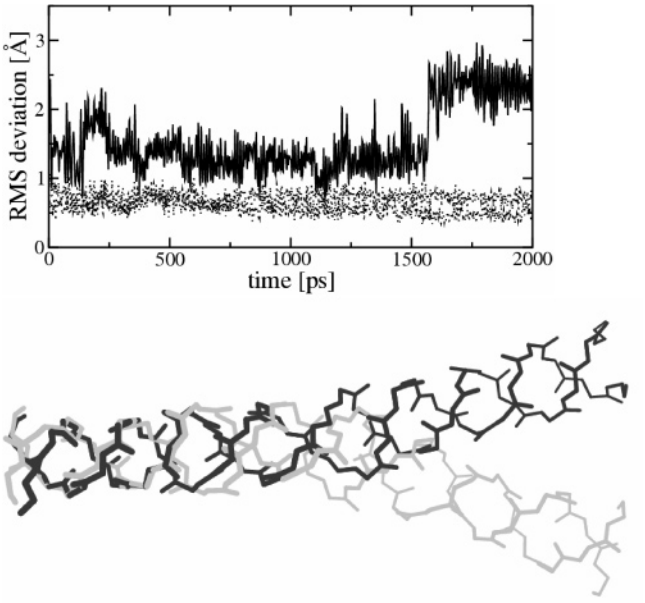

Figure 4. Top panel: Root-mean-square deviation of the dimer molecule from MD simulations at $T = 300$ K. The solid line is the rms deviation of the entire molecule, and the dashed lines represent rms deviations separately from one-half of the double helix. The second half exhibits the same behavior (rms deviations not shown). Only backbone atoms are considered. Bottom panel: Superposition of the initial (dark gray) and final (light gray) snapshots of the MD trajectory, showing the bending of the double helix. The figure was generated using MOLSCRIPT.[29]

The time evolution of the rms deviation relative to the initial energy-minimized conformation of the double-stranded dimer is shown in Figure 4. The rms deviations show large fluctuations, which indicate a structural transition at about 1.5 ns. These deviations are due to global oscillatory bending motions at the succinate linker involving the two halves of the double helix structure. The transition occurring at 1.5 ns corresponds to a persistent bending of the two halves of the double helix. Nevertheless, the conformation of each half double helix is largely conserved during the MD simulation. For all four single-helical strands, which are paired to form the two halves of the double helix, the rms deviations are below 1 Å, as one can infer from Figure 4. Thus, we can conclude that, although the oscillations in the orientation result in large rms deviations of the dimer structure, the stability of the helical regions is not affected. The same results, namely, bending oscillations of the two halves of the dimer molecule and low rms deviation for each half of the double helix, are also observed in the other 9 trajectories (data not shown).

The time evolution of the monomer structure was simulated under the same conditions as the dimer structure for 10 trajectories. We selected 1 trajectory of a 2 ns time length that can demonstrate the typical dynamical behavior of the monomer structure in the absence of ions. The rms deviations based on this trajectory are shown in Figure 5. Similarly as for the MD

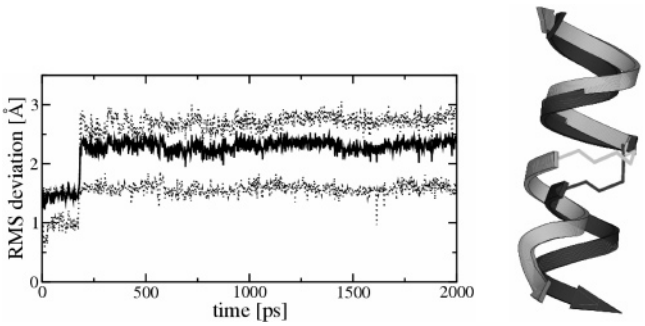

Figure 5. Left panel: Root-mean-square deviation of the monomer structure simulated at $T = 300$ K in the absence of ions. The solid line depicts the rms deviation of the entire molecule, and the dashed lines represent rms deviations of the two halves of the helix connected by succinate. Right panel: Ribbon representation of the monomer structure after 2 ns (light gray), to be compared with the initial structure (dark gray). The figure was generated using MOLSCRIPT.[29]

simulation of the dimer (Figure 4), the rms deviation of the monomer structure increases rapidly in particular in the first 50 ps to 1.5 Å. At around 200 ps, a transition occurs, involving one-half of the single-stranded helix. The rms deviation of this half shows a significant increase, revealing a structural change. Visualizing the time evolution of the monomer structure for this trajectory, one observes that at this point the terminal helix turn is losing its initial shape and fraying and both helix halves are bent at the linker (Figure 5, right panel). After about 50 ps, the other half of the helix is reaching an rms value, which is significantly larger than the corresponding value obtained considering each single-helical strand of the dimer structure separately. Although such a significant change in monomer structure is observed only in 4 out of 10 trajectories, the remaining 6 trajectories exhibit also a high degree of flexibility particularly in the helix ends. While the rms deviations for each half of the dimer structure are smaller than 1 Å (Figure 4), the corresponding value for the monomer structure is typically around 2−3 Å (data not shown). Thus, the rms deviation analysis suggests that in the absence of ions the monomer structure is easily destabilized while the dimer structure maintains to a large extent the helical conformation. This is compatible with what is actually observed in experiments in ref 16.

Stabilizing Effect of Two Bound Cs^+ Ions. In experiments, the addition of CsI to the solution stabilizes the monomer structure. This might be due either to an increase in ionic strength, which can shield unfavorable electrostatic interactions, or to a specific ion binding as suggested in ref 16. In an MD simulation of the monomer structure for 2 ns using the generalized Born solvent approximation with an ionic strength of 1 M, the rms deviations increased similarly as in the absence of ions, thus suggesting that the bare ionic strength is not responsible for a stabilization of the monomer structure (Figure 6).

Inserting two explicit Cs^+ ions into the monomer structure, as described in the Materials and Methods section, leads to a stabilization of the monomer structure. This is shown in the analysis of rms deviations for a set of 10 MD trajectories of 1 ns each, obtained at $T = 300$ K and at an implicit ion concentration of 1 M. As pointed out in the Materials and Methods section, changing the implicit ionic strength does not affect the structural changes observed for monomer and dimer structure during MD simulation. These changes are the increase of rms deviation of the monomer structure without explicit ions as compared to the monomer structure with two Cs^+ ions

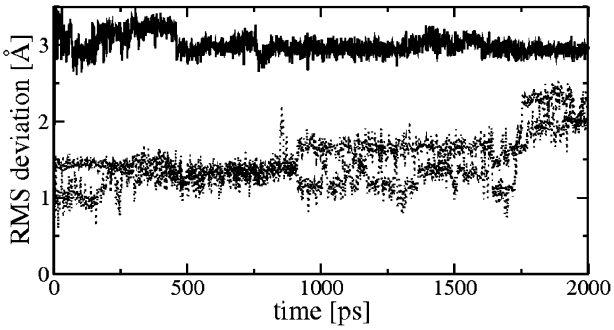

Figure 6. Root-mean-square deviations of the monomer structure, when simulated at 1 M ion concentration and $T = 300$ K, without explicit ions. Solid and dashed lines as in Figure 5.

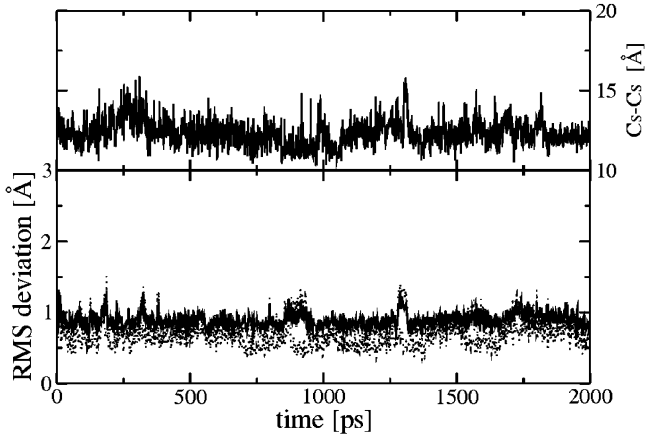

Figure 7. Root-mean-square deviation from the starting structure of the monomer at $T = 300$ K with two Cs^+ ions placed into the channel. The ionic strength is set to 1 M. Top plot: Time evolution of the Cs^+ ion pair distance. Bottom plot: The solid line represents the rms deviation of the entire monomer, whereas dashed lines represent the rms deviations of the two helix halves.

inserted at both channel ends. The ionic strength of 1 M was chosen for the MD simulation because at this value the high ion conductivity of the synthetic gramicidin ion channel was observed experimentally, which corroborates with the two Cs^+ ion binding sites suggested form the NMR structure.[16] Again, a single trajectory of 2 ns time length is chosen for a more detailed representation of the results (Figure 7), albeit data from the other 9 trajectories that were also analyzed showed the same behavior. The MD simulation was started after optimizing the positions of the two Cs^+ ions, placed in the channel, by means of an energy minimization in the presence of the implicit solvent model (Materials and Methods). Although the repulsive interaction between the two Cs^+ ions is generating some additional fluctuations in the rms deviation (Figure 7, bottom panel), both ions remain in the channel during the simulation, and the backbone rms deviation of the two helix halves remains around 1 Å or below. If we compare this plot with Figures 4 and 5, then we can conclude that the Cs^+ ions reduce the increase of rms deviation from the initial NMR structure and thus provide a stabilizing effect, interacting with the backbone oxygens mainly at the entrance of the channel and also with the terminal ethanolamine oxygen. This is clear also from the analysis of the remaining 9 trajectories. Although the central region of the helix is rigid in both configurations so far presented, namely, the monomer structure with ions and the monomer structure without ions, visible differences arise at chain ends, which are much less conserved during MD simulations of the monomer structure without bound Cs^+ ions. The effect of the bound Cs^+

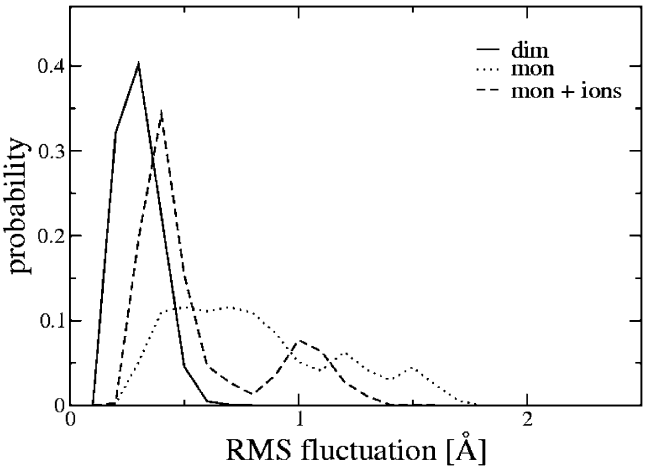

Figure 8. Fluctuations of single-helical strands of the monomer and dimer structures with solute and solvent dielectric constants of $\epsilon = 4$ and $\epsilon = 20$, respectively, at $T = 300$ K. The fluctuations are evaluated as histograms of the rms deviations from the average structure. The two helical parts of each polypeptide chain were considered separately by excluding the linker region. To generate the histogram, atomic coordinates of the MD simulation data were taken every 2 ps from all 10 trajectories each of 1 ns time period. For each set of coordinates, averaged over all backbone atoms, the rms deviations from the average structures of the two (monomer) or four (dimer) helical strands were calculated and sampled in the histogram, which was finally normalized. The average structure used as reference was calculated for the 10 trajectories. We observed that the dimer (solid line) has low rms fluctuations, while the monomer structures exhibit larger rms fluctuations (dotted line) but are stabilized by the addition of two Cs^+ ions at both ends (dashed line).

ions is to keep the ends of the molecule in place, thus avoiding unwinding of the helix.

Evaluating the probability distribution of rms fluctuations of the monomer and dimer structures based on the MD simulations of all 10 of the 1 ns trajectories, we observed values well below 0.5 Å for the dimer structure, considering the helical parts separately while ignoring the linker part (solid line in Figure 8). These small fluctuations correspond to very rigid structures. In contrast, the monomer structure is comparatively much more flexible, with rms fluctuations that are significantly above 0.5 Å with side maxima at 1.2 and 1.5 Å (dotted line in Figure 8). This is related to the observed instability of the terminal part of the helices. Interestingly, when the Cs^+ ion pair is added, the monomer structure becomes nearly as rigid as the dimer structure, exhibiting a side peak at 1 Å (dashed line in Figure 8).

Simulation of the Monomer Structure in the Presence of Explicit Ions: Cs^+ Ion Binding. The initial monomer structure was put into an ionic bath, consisting of a random distribution of 157 Cs^+ atoms with charge +1 and twice the number of counterions, with charge −0.5 to keep the system charge neutral. Van der Waals radii were defined as described in the Materials and Methods section. The amount of charges in the ionic bath corresponds to an ionic strength of 2 M. We used the implicit solvent model with a dielectric constant $\epsilon = 20$ as in the previous MD simulations. We generated 10 trajectories of 2 ns time length each. Besides calculating the time evolution of rms deviations, we focused in this analysis on the Cs^+ ion binding reaction monitoring the motion of Cs^+ ions in the vicinity of the channel pore. We observed for all 10 MD simulations that two Cs^+ ions moved quickly (in all cases within the first 50 ps) from the bulk of the solution toward the channel entrances on both sides, where they persisted at a distance of about 9 Å from the channel center. The subsequent events depend on the trajectory and can be classified in three groups, which are listed below:

In 3 trajectories, one Cs^+ ion enters the channel where it binds for a duration of several tens of picoseconds before it is released again.

In 5 trajectories, one Cs^+ ion enters the channel and is bound at a distance of about 5 Å from the channel center, where it remains until the end of the simulation (typically several hundred picoseconds).

In 2 trajectories, after binding of the first Cs^+ ion at one channel pore, a second Cs^+ ion enters the pore at the opposite channel end and binds at a distance of about 12 Å from the first ion. Both ions remain bound until the end of the simulation.

The analysis of MD simulation data that are presented here in detail considers one of the latter two trajectories where two Cs^+ ions bind in the channel. The first Cs^+ ion is bound after 50 ps, being attracted by three backbone oxygens belonging to three D-leucine residues in the first helical turn. The second Cs^+ ion remains close to the channel entrance on the opposite side and interacts with the closest carbonyl oxygen atoms of the D-leucine residuces as well and with the oxygen of the terminal ethanolamine. After about 900 ps, the ethanolamine moves away, and the second Cs^+ ion enters the channel pore. These events are shown in the snapshots given in Figure 9. They can also be related to steps appearing in the time evolution of the pair distance of the two Cs^+ ions that are going to bind in the channel (upper plot in Figure 10).

The analysis of the MD simulation data (Figure 10) reveals that the monomer structure is stabilized after binding of the first Cs^+ ion, just after an initial increase of rms deviation. While the binding reaction of the second Cs^+ ion takes place, the first ion remains in the same position. Although the two Cs^+ ions keep the rms deviation of the two helical halves of the polypeptide below 1 Å (Figure 10, bottom plot), their presence results in larger local fluctuations, which increase while the distance between the two Cs^+ atoms decreases to about 1.3 ns.

Discussion

Comparison between the Monomer and Dimer Structures. Our MD simulation data showed that the dimeric form of the synthetic polypeptide that mimics mini-gramicidin A does not undergo structural changes on the simulation time scale of 2 ns, which may suggest that the structure is stable in isotropic solution without ions. Nevertheless, the molecular structure obtained in the MD simulation is bent at the succinate linker and performs bending oscillations, thus deviating from the average minimized NMR structure. Interestingly, the bending oscillation does not affect the structure of both halves of the double helix, which remain close to the starting structure, showing an rms deviation generally below 1 Å (Figure 4).

The monomer structure instead shows larger rms deviations from the NMR structure, which indicates a more pronounced instability. In 4 out of 10 trajectories, the monomer performs rapidly a structural transition, which involves one-half of the helix. This transition consists of bending at the succinate linker and of deformation of the terminal helical turn, the pore radius locally decreases, and the channel loses partially its helical form, which indicates that the proposed NMR structure cannot exist in the absence of ions. The stabilizing effect of Cs^+ ions is confirmed by the set of simulations with two ions placed into the channel, whose presence keeps the monomer structure close to the initial conformation. So far, we can conclude that the proposed mechanism for the dimer to monomer transition[16]

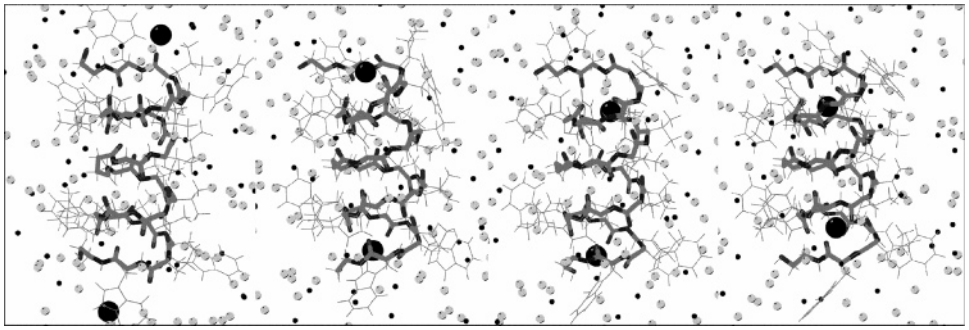

Figure 9. Four snapshots from the MD simulation of the synthetic ion channel in the presence of explicit ions. From left to right, conformations at 0 ps (initial conformation), 50 ps, 200 ps, and at 1 ns are shown. Cs^+ ions are depicted as small dark gray spheres, and the positive ions are the light gray spheres. The two Cs^+ ions involved in the binding events are highlighted using a larger sphere radius. The figure was generated using MOLSCRIPT.[29]

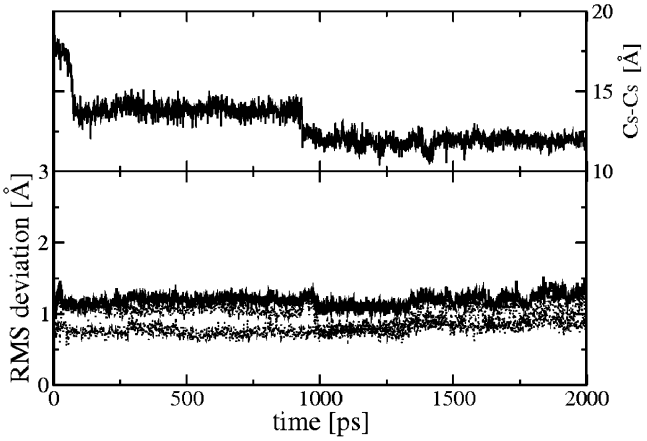

Figure 10. MD simulation of the monomer structure with explicit ions. Top plot: Time evolution of the Cs^+ ion pair distance referring to the two Cs^+ ions, which are bound to the channel during the MD simulation. Bottom plot: Root-mean-square deviation of the entire molecule (solid black line) and of the two helix halves (dashed lines).

requires indeed the presence of Cs^+ ions for the monomeric structure to exist. However, the destabilization of the dimer structure due to Cs^+ ions remains an open issue. The transition may be very slow and therefore require much longer time scales to be observed in MD simulations.

The question arises whether the presence of the positive charges of two Cs^+ ions is essential to stabilize the monomeric channel structure. In fact, according to the specific channel geometry characterized by the orientation of the backbone oxygen atoms that point toward the cavity center, a positive charge is useful to stabilize the channel structure. Alternatively, the stabilization might also be achieved by polar groups that are placed in the channel cavity. A test MD simulation where the two Cs^+ ions were replaced by two explicit water molecules showed a quite different behavior. Now the monomer fluctuations are comparable to the ones presented in Figure 6. In contrast to the two well-localized Cs^+ ions, the water molecules are relatively mobile and travel along the channel axis.

During the modeling of the monomer structure with the two bound Cs^+ ions, we observed that a single Cs^+ ion, positioned outside of the channel or in the interior, is easily attracted to a binding site positioned on the channel axis at about 5−6 Å from the channel center by means of a short minimization (Materials and Methods section). Thus, there is practically no energy barrier for a Cs^+ ion to enter the channel. This is likely to be an artifact of the implicit solvent model used in the present application. Explicit solvent, even of moderate polarity, would provide a locally structured dielectric environment induced by the presence of an ion. This specific solvent polarization would lower the ion solvation energy and result in an energy barrier when the ion leaves the bulk solvent to enter the ion channel.[30] Preliminary computations with explicit solvent are in progress and seem to confirm this picture.

The shape of the potential energy profile in the channel interior is characterized by minima and maxima that allow the ion to move along, coming closer to the picture of a uniform Cs^+ ion potential energy along the channel axis.[30] Our data qualitatively agree with other theoretical results obtained with a solvent model using continuum electrostatics.[11] It was suggested that modeling the solvent by continuum electrostatics might not be suitable to obtain quantitatively correct predictions on ion flow through a polypeptide channel, because of a lack of detailed microscopic interactions between the polypeptide and water molecules within the narrow ion channel, which might affect the channel potential.[11] However, semimicroscopic approaches with implicit solvent were successful in addressing questions related to energetics, ion selectivity, and flow.[31−33] In the present study, we do not focus on simulating ion permeation but rather investigate stability properties of the synthetic mini-gramicidin A channel; thus, we consider the implicit solvent model to be appropriate.[34] The binding sites that we found for the Cs^+ ions are in agreement with those derived from analysis of NMR data on Na^+ binding to native gramicidin ion channels.[34]

Cs^+ Ion Binding Reaction. In the previous paragraph, we discussed the stabilization induced by Cs^+ ions bound in the channel formed by the single-helical monomer of the synthetic mini-gramicidin A. Here, we focus on the binding reaction as it occurs spontaneously in our dynamic simulation. As suggested from the experiments in ref 16, we found that the monomer structure consisting of the single-stranded helix is promptly binding a Cs^+ ion in the majority of cases after few tens of picoseconds of MD simulation. The binding reaction for the second ion is more rare, as can be expected because of the electrostatic repulsion between the two positive charges of the Cs^+ ions, but still it is detected in 2 out of 10 short MD trajectories of 1 ns in time span. We observed that the binding of the second Cs^+ ion caused some increase in fluctuations (Figure 10) although both Cs^+ ions remain in their places. Theoretical studies on ion permeation of gramicidin channels show that multiple occupancy is favored for larger cations such as Cs^+.[35] This agrees with our MD simulation results, explaining why the binding of the second Cs^+ ion also occurs quite efficiently. A very high permeability for the Cs^+ ions was observed also in several other preliminary MD simulations, which were performed at a lower concentration of explicit ions, corresponding to an ionic strength of about 0.3 M. There, in two cases, we even detected the binding of three Cs^+ ions. In

one case after binding of two Cs^+ ions in the channel, the channel pores were capturing more Cs^+ ions at both ends.

To investigate a possible destabilization of the dimer structure induced by Cs^+ ions, which would trigger the dissociation reaction leading to the formation of the monomer structure, we also generated a set of 10 trajectories for the dimer, each of a 1 ns time span. Thereby, we used the same conditions for the MD simulation employed to study the stability of the monomer structure. Unfortunately, no remarkable destabilization was observed on the time scale of 1 ns. A possible explanation is that the dissociation occurs on much longer time scales and thus cannot be detected.

Conclusions

The set of MD simulations on both conformations of the synthetic gramicidin-like channel confirms to a large extent the results that were obtained and suggested from experiments. Namely, the dimer structure is stable in the absence of Cs^+ ions, whereas the monomer structure is extremely flexible without ions but is stabilized after the binding of two Cs^+ ions at both ends of the synthetic ion channel. This effect was observed both by placing the two Cs^+ ions at optimal positions in the channel before performing MD simulations as well as by placing the channel molecule in solvent modeled by a dielectric medium with explicit ions. In the latter case, a Cs^+ ion entered the channel from both sides spontaneously after a few picoseconds. These results give further insight into the properties of synthetic peptide channels, providing a useful complement to experiments. The simulation of current flow through ionic channels by means of all-atom molecular dynamics is still a hard task[10,34,36] due to the complexity and large size of the models (channel embedded in a lipid bilayer with explicit solvent) and the intrinsic time length of the process, which is typically in the range of microseconds. Yet, there is a wide range of application for computer simulations with implicit solvent, including also molecular dynamics, which can be successfully used to understand and predict a number of features of synthetic ion channels, as is demonstrated in the present work.

Acknowledgment. We are grateful for helpful discussions with Dr. Milan Hodoscek. This project was supported by the Deutsche Forschungsgemeinschaft SFB 498, Project A5, Forschergruppe, Projects KN 329/5-1/5-2, GRK 80/2, GRK 268/2, and GKR 788/1, the Fonds der Chemischen Industrie, and the BMBF.

Supporting Information Available: Charges for ethanolamine, rms fluctuations of single-helical strands of monomer and dimer structures, and rms devation of the monomer and dimer structures with respect to the starting conformation. This material is available free of charge via the Internet at http://pubs.acs.org

References and Notes

(1) Dubos, R. J.; Hotchkiss, R. D. *J. Exp. Med.* **1941**, *73*, 629.
(2) Bourinbaiar, A. S.; Krasinski, K.; Borkowsky, W. *Life Sci.* **1994**, *54*, PL5.
(3) Hladky, S. B.; Haydon, D. A. *Biochim. Biophys. Acta* **1972**, *274*, 294.
(4) Veatch, W. R.; Fossel, E. T.; Blout, E. R. *Biochemistry* **1974**, *13*, 5249.
(5) Pascal, S. M.; Cross, T. A. *J. Biomol. NMR* **1993**, *3*, 495.
(6) Zhang, Z. L.; Pascal, S. M.; Cross, T. A. *Biochemistry* **1992**, *31*, 8822.
(7) Kovacs, F.; Quine, J.; Cross, T. A. *Proc. Natl. Acad. Sci. U.S.A.* **1999**, *96*, 7910.
(8) Allen, T. W.; Andersen, O. S.; Roux B. *J. Am. Chem. Soc.* **2003**, *125*, 9868.
(9) Bingham, N. C.; Smith, N. E. C.; Cross, T. A.; Busath, D. D. *Biopolymers* **2003**, *71*, 593.
(10) Allen, T. W.; Andersen, O. S.; Roux B. *Proc. Natl. Acad. Sci. U.S.A.* **2004**, *101*, 117.
(11) Edwards, S.; Corry, B.; Kuyucak, S.; Chung, S. H. *Biophys. J.* **2002**, *83*, 1348.
(12) Kuyucak, S.; Andersen, O. S.; Chung, S. H. *Rep. Prog. Phys.* **2001**, *64*, 1427.
(13) Åqvist, J.; Warshel, A. *Biophys. J.* **1989**, *56*, 171.
(14) Elber, R.; Chen, D. P.; Rojewska, D.; Eisenberg, R. *Biophys. J.* **1995**, *68*, 906.
(15) Koeppe II, R. E.; Andersen, O. S. *Annu. Rev. Biophys. Biomol. Struct.* **1996**, *25*, 231
(16) Arndt, H. D.; Bockelmann, D.; Knoll, A.; Lamberth, S.; Griesinger, C.; Koert U. *Angew. Chem.* **2002**, *114*, 4234.
(17) Roux, B.; Karplus, M. *Annu. Rev. Biophys. Biomol. Struct.* **1994**, *23*, 731.
(18) Brooks, B. R.; Bruccoleri, R. E.; Olafson, B. D.; States, D. J.; Swaminathan S.; Karplus, M. *J. Comput. Chem.* **1983**, *4*, 187.
(19) MacKerell, J., A. D.; Bashford, D.; Bellott, M.; Dunbrack, R. L., Jr.; Evanseck, J.; Field, M. J.; Fischer, S.; Gao, J.; Guo, H.; Ha, S.; Joseph, D.; Kuchnir, L.; Kuczera, K.; Lau, F. T. K.; Mattos, C.; Michnick, S.; Ngo, T.; Nguyen, D. T.; Prodhom, B.; Reiher, I., W. E.; Roux, B.; Schlenkrich, M.; Smith, J.; Stote, R.; Straub, J.; Watanabe, M.; Wiorkiewicz-Kuczera, J.; Yin, D.; Karplus, M. *J. Phys. Chem. B* **1998**, *102*, 3586.
(20) Bayly, C. I.; Cieplak, P.; Cornell, W. D.; Kollmann P. A. *J. Phys. Chem.* **1993**, *97*, 10269.
(21) Nose, S. *J. Chem. Phys.* **1984**, *81*, 511
(22) Hoover, W. G. *Phys. Rev. A* **1985**, *31*, 1695.
(23) Still, W. C.; Tempczyk, A.; Hawley, R. C.; Hendrickson, T. *J. Am. Chem. Soc.* **1990**, *112*, 6127.
(24) Im, W.; Lee, M.; S., Brooks, C., III L. *J. Comput. Chem.* **2003**, *24*, 1691.
(25) Warshel, A.; Russell S. T. *Q. Rev. Biophys.* **1984**, *17*, 283.
(26) Simonson, T.; Brooks, C. L., III *J. Am. Chem. Soc.* **1996**, *118*, 8452.
(27) Sayle, R.; Milner-White, E. J. *Trends in Biochem. Sci.* **1995**, *20*, 374.
(28) Pearlman, D. A.; Case, D. A.; Caldwell, J. W.; Ross, W. S.; Cheatharm, T. E., III; De Bolt, S.; Ferguson, D.; Seibel, G.; Kollmann, P. *Comput. Phys. Commun.* **1995**, *91*, 1.
(29) Kraulis, P. J. *J. Appl. Crystallogr.* **1991**, *24*, 946.
(30) Jordan, P. C. *Biophys. J.* **1990**, *58*, 1133.
(31) Chung, S. H.; Kuyucak S. *Eur. J. Biochem.* **2002**, *31*, 283.
(32) Burykin, A.; Schutz, C. N.; Villa, J.; Warshel, A. *Proteins* **2002**, *47*, 265.
(33) Burykin, A.; Kato, M.; Warshel, A. *Proteins* **2003**, *52*, 412.
(34) Roux, B. *Acc. Chem. Res.* **2002**, *35*, 366.
(35) Roux, B.; Prodhom, B.; Karplus, M. *Biophys. J.* **1995**, *68*, 876.
(36) De Groot, B. L.; Grubmüller, H. *Science* **2001**, *294*, 2353.